

Article

A Nourishment Performance Index for Beach Erosion/Accretion at Saadiyat Island in Abu Dhabi

Waleed Hamza ¹, Giuseppe Roberto Tomasicchio ² , Francesco Ligorio ², Letizia Lusito ^{2,*} 
and Antonio Francone ³

¹ Biology Department, College of Science, United Arab Emirates University, 15551 Al Ain, UAE; w.hamza@uaeu.ac.ae

² Department of Engineering for Innovation, University of Salento, Ecotekne, 73100 Lecce, Italy; giuseppe.tomasicchio@unisalento.it (G.R.T.); francesco.ligorio@unisalento.it (F.L.)

³ Department of Civil Engineering, University of Calabria, 87036 Arcavacata di Rende (CS), Italy; antonio.francone@unical.it

* Correspondence: letizia.lusito@unisalento.it

Received: 20 April 2019; Accepted: 29 May 2019; Published: 1 June 2019



Abstract: The present paper proposes a methodology to optimise the design of a beach protection intervention at Saadiyat Island, of the Abu Dhabi city in the United Arab Emirates. In particular, a nourishment performance index (NPI) has been introduced to select among different design alternatives of a coastal engineering intervention related to the ongoing development of the island. The NPI is based on general factors such as the initial volume of sand necessary for the nourishment, the beach surface loss after the intervention and the closure depth. The proposed index, properly integrated with a numerical simulation of the beach morphodynamics, is shown to be promising in the evaluation of the feasibility for the planned coastal defence interventions. The adoption of different design scenarios has showed that the NPI value depends mainly on the built nourishment shoreline.

Keywords: beach morphology; beach nourishment performance; sustainable development; General Shoreline beach model; United Arab Emirates; Saadiyat Island

1. Introduction

In the present paper, the definition of a nourishment performance index (NPI) for coastal engineering interventions is proposed, based only on general factors such as the initial sand volume necessary for the nourishment, the beach surface loss after the intervention and the closure depth (defined in [1]), which indicates the seaward depth limit to the active profile.

In particular, the NPI has been determined for a coastal prediction system to be built at Saadiyat beach, in Saadiyat Island, a large low-lying 27 km² island situated in the Arabian Gulf (also named Persian Gulf) within the Emirate of Abu Dhabi of the United Arab Emirates (Figure 1). Saadiyat Island comprises a SW–NE oriented, 9 km long natural sandy beach, Saadiyat beach, of moderate to flat slope. The shape and orientation of the beach has been modified several times for the development of the Cultural District of Saadiyat Island. The present study focuses on the western area of Saadiyat beach, a 2 km long beach. Where the urban plan requires the realization of sustainable coastal protection structures, different design scenarios have been proposed by the Tourism Development Investment Company (TDIC), described in the relative TDIC master plan. According to the last development plan as approved by TDIC, the intervention for Saadiyat beach involves a large sand nourishment intervention and the construction of four groyne; the number and location of the four groyne has been decided by TDIC and no contribution from the present Authors has been given.



Figure 1. Top: view of the Arabic Gulf area showing the position of Abu Dhabi; bottom: aerial view of Saadiyat island, in the Abu Dhabi Municipality; the red rectangle indicates the position of the Saadiyat beach study area.

In order to quantify the feasibility for each of the design scenarios developed by TDIC, a deep knowledge of the engineering details and the coastal conditions, such as the performance of the intervention, the morphodynamics response of the shoreline to the various different coastal defence scenarios of the TDIC development plan is required [2–5].

The objective of the present study is to identify a methodology to evaluate the nourishment performance for different scenarios of coastal defence at Saadiyat beach. The proposed methodology is based on the recent availability of observational data (i.e., data measured by in-situ instruments, see Sections 2.1 and 2.2, and data recorded by remote observing systems like satellites, see Section 2.3.3), allowing to define with precision the wave climate (the distribution of wave characteristics averaged over a period of time and for a particular location) and coast landforms, i.e., any of the relief features present along the coast, which are the result of a combination of processes, sediments and the geology of the coast itself. The observational data were collected by means of in-situ monitoring instruments, survey campaigns and satellite imagery. The data collection has served as a basis for numerical models-based simulations of the oceanographic conditions (wave climate) and of the morphological changes in the natural shape of the coastline under the influence of the planned

interventions. The outcomes of the performed numerical simulations allow the identification of the more environmentally sustainable scenario for Saadiyat beach.

2. Materials and Methods

The proposed methodology is based on the collection of observational data and the use of numerical models in a joint way.

2.1. Sediment Characteristics

Within a survey campaign in May 2017, different sediment samples have been collected at points indicated in Figure 2 and Table 1 with water depths ranging from 1 m to 3 m. The samples indicated as 8 and 9 have been collected at the same time with few meters distance from each other. The concentration of each granulometric fraction was obtained through a sieve analysis with the corresponding results reported also in Table 1.



Figure 2. Location of sediment samples.

Table 1. Sediment characteristics of Saadiyat beach: coordinates and water depths of collection points, sample weight percentages passing different meshes (of sizes 5 μm, 10 μm and so on), corresponding D₅₀ values and, finally, sand classification according to [6].

| ID | Location | | Water Depth (m) | Weight (%) Passing Each Mesh (μm) | | | | | | | | Sand Classification | |
|----|-------------|-------------|-----------------|-----------------------------------|-------|-------|-------|-------|--------|--------|---------|----------------------|--------|
| | Coordinates | | | 5 μm | 10 μm | 18 μm | 35 μm | 60 μm | 120 μm | 230 μm | >230 μm | D ₅₀ (mm) | Type |
| 1 | 54°23'10" E | 24°32'18" N | 2 | - | 0.4% | 0.4% | 12.2% | 61.8% | 22.0% | 2.3% | 0.9% | 0.44 | Medium |
| 2 | 54°25'20" E | 24°32'40" N | 2 | - | 0.2 | 1.0 | 4.2 | 14.7 | 63.1 | 16.1 | 0.7 | 0.26 | Medium |
| 3 | 54°24'07" E | 24°32'31" N | 2 | - | 0.2 | 0.5 | 5.2 | 30.3 | 61.3 | 1.6 | 0.9 | 0.33 | Medium |
| 4 | 54°24'55" E | 24°32'42" N | 2 | - | 0.0 | 0.1 | 1.8 | 17.8 | 71.1 | 8.6 | 0.6 | 0.27 | Medium |
| 5 | 54°25'43" E | 24°33'02" N | 3 | - | 0.5 | 7.0 | 33.5 | 49.0 | 9.3 | 0.4 | 0.3 | 0.65 | Coarse |
| 6 | 54°25'53" E | 24°32'52" N | 1 | - | 0.3 | 1.4 | 7.5 | 37.7 | 40.8 | 11.4 | 0.9 | 0.34 | Medium |
| 7 | 54°26'39" E | 24°33'24" N | 2 | - | 0.1 | 0.2 | 0.6 | 1.0 | 34.8 | 59.8 | 3.5 | 0.16 | Fine |
| 8 | 54°26'52" E | 24°33'39" N | 2 | - | 0.3 | 0.4 | 0.9 | 7.2 | 27.1 | 57.7 | 6.4 | 0.16 | Fine |
| 9 | 54°26'52" E | 24°33'39" N | 2 | - | 0.1 | 0.5 | 2.1 | 9.5 | 59.5 | 27.7 | 0.6 | 0.22 | Fine |
| 10 | 54°26'57" E | 24°33'35" N | 2 | - | 0.0 | 0.4 | 2.2 | 32.3 | 54.7 | 9.9 | 0.5 | 0.30 | Medium |

Table 1 shows also the value of the mean diameter of the sediment sample, D₅₀ (given in mm) and the classification of the beach type according to [6] at each collection point.

Although important for a complete sedimentological mapping of the area, it was not possible to gain information on the textural characteristics of sand [7–9].

2.2. Local Wave Climate

Direct wave measurements are considered the most reliable source of information. In the Gulf area, this type of information is rare or even missing. However, recently, in vicinity of Saadiyat beach, the Abu Dhabi Municipality (ADM) installed two Argonaut-XR ADCP (Acoustic Doppler Current Profiler) produced by the company “SonTek—A Xylem Brand” (San Diego, CA, USA) to observe the atmospheric and oceanographic conditions (water level, significant wave height, peak wave period, water temperature and wind speed and direction). Courtesy of the ADM, this observations dataset was made available. The coordinates of the positions of the two instruments and the relative water depth are reported in Table 2. The data from instrument “04” present a very high percentage of data gaps and they have not been analysed. The recorded data from instrument “03”, indicated as *ADMins* in the following, span the period from June 2015 to January 2018 (included), with a time resolution of 10 min and 30 min for the atmospheric and oceanographic variables, respectively [10]. The percentage of data gaps is around 4.5%, keeping into account that the instrument did not work for a time equal to around 42 days in total in the entire period June 2015–January 2018. Data successfully collected have been considered of good quality, since the quality control is ensured by the robustness of the native software/data acquisition system of the Argonaut-XR. Figure 3 shows the location of the *ADMins*. In addition, Figure 3 shows also the grid node of the NOAA (National Oceanic and Atmospheric Administration, a scientific agency within the United States Department of Commerce) offshore wave data (coordinates 25° N and 54° E, 16 m water depth) used to calculate the closure depth (Section 2.3.3).

Table 2. Coordinates of the positions of the two instruments installed by the Abu Dhabi Municipality (ADM) and the relative water depth.

| Instrument | Longitude (E) | Latitude (N) | Water Depth (m) |
|----------------------|---------------|--------------|-----------------|
| 03 (<i>ADMins</i>) | 54°24′29.52″ | 24°34′17.04″ | 6 |
| 04 | 54°16′39.72″ | 24°44′31.56″ | 18 |



Figure 3. Location of *ADMins*, and NOAA nearshore and offshore grid points for the wind/wave model data.

The NOAA National Centers for Environmental Prediction (NCEP) developed the Climate Forecast System (CFS), a fully coupled model representing the interaction between the Earth’s atmosphere, oceans, land and sea ice. A reanalysis of the sea and atmosphere state for the period of 1979–2009 has been conducted, resulting in the CFS Reanalysis (CFSR) dataset [11]. The vertical discretization

of the atmosphere consists of 64 layers. The temporal resolution for the atmospheric variables is 3 h. Using the CFSR dataset, the NOAA Marine Modeling and Analysis Branch (MMAB) has produced a wave hindcast for the same period. The wave hindcast dataset has been generated using the WAVEWATCH III (WW3) model (v3.14), and it is suitable for use in climate studies. The wave model suite consists of global and regional nested grids. The rectilinear grids have been developed using ETOPO-1 bathymetry [12], together with v1.10 of the Global Self-consistent Hierarchical High-resolution Shoreline (GSHHS) database. The spatial resolution of the considered data is $1/6^\circ$, which corresponds to roughly 20 km. The North West Indian Ocean computational grid, adopted in the considered data, extends in longitude from 30° E to 70° E (with 241 grid nodes) and in latitude from 20° S to 31° N (307 grid nodes). The NOAA datasets (both wind and waves) are freely available. The NOAA WAVEWATCH III/CFSR webpages [13,14] present additional details about the datasets.

2.3. Morphodynamic Modelling Techniques

2.3.1. Overview of Popular Commercial Software

A large and growing number of models have been developed to compute the morphodynamic evolution of coastal environments. These span a large range of process combinations, scales and levels of detail. The majority of existing large-scale coastline models address sandy coastline evolution. The spatial scales addressed in these models range from meters to kilometres while temporal scales range from hours to decades. The smaller space and time scale models typically employ explicitly reductionist methodologies where conservation of momentum forms the explicit means for evolving the system [15,16]. These models are typically used to simulate response from specific forcing events. Belonging to this category, XBeach [17] uses conservation of momentum and advection diffusion equations for sediment transport to simulate the response of the coast and dune to individual storm events. Larger scale models use a range of approaches to evolve system characteristics. On the contrary, GENESIS (GENeralized model for Simulating Shoreline change) [18], is designed to simulate long-term shoreline change at coastal engineering projects as produced by spatial and temporal changes in longshore sand transport. Typical longshore extents and time periods of modelled projects can be in the ranges of 1 to 100 km and 1 to 100 months, respectively, and almost arbitrary numbers and combinations of groins, detached breakwaters, seawalls, jetties and beach fills can be represented.

The model called Cascade [19] was developed to simulate regional sediment transport and coastal evolution. Representation of inlets is of special interest in how they function in the regional sediment transport system in terms of storing and transferring sediment, with consequences for the adjacent beaches. In Cascade, the coupling between the regional and local scale occurs in a hierarchical manner, that is, information is supplied from the regional scale to the local scale.

GenCade (from the combination of the words "Genesis" and "Cascade") [20] is a newly developed numerical model, which combines the engineering power of GENESIS and the regional processes capability of the Cascade model. The main utility of the modelling system lies in simulating the response of the shoreline to structures sited in the nearshore. Shoreline change produced by cross-shore sediment transport as associated with storms and seasonal variations in wave climate cannot be simulated.

The model LITPACK is developed by the Danish Hydraulic Institute (DHI) and it requires a commercial license [21]. LITPACK consists of an integrated system of modelling of coastal processes and dynamics of the coastline, capable to manage interventions in the coastline such as optimisation of beach creations and coastal protection interventions, impact assessments of coastal constructions.

Within the Delft3D modelling package, a large variation of coastal and estuarine physical and chemical processes can be simulated [22]. These include waves, tidal propagation, wind- or wave-induced water level setup, flow induced by salinity or temperature gradients, sand and mud transport, water quality and changing bathymetry (morphology). Delft3D is a very powerful Open Source Software, but its range of applications go far beyond the beach morphology evolution modelling

that is required in the present work. Therefore, the shoreline evolution simulation has been performed by means of the General Shoreline beach (GSb) model.

2.3.2. GSb Model Description

Numerical simulations have been conducted by means of a newly proposed morphodynamic model, named General Shoreline beach 1.0 (GSb), belonging to the one-line model typology [23]. This typology assumes that the beach cross-shore profile remains unchanged [24,25], thereby allowing beach change to be described uniquely in terms of the shoreline position. The peculiarity of the GSb model consists of simulating shoreline evolution based on a longshore transport formula/procedure suitable at any coastal mound: sand, gravel, cobbles, shingle and rock beaches [26–32]. It is mainly based on the General Longshore Transport (GLT) model as in [28], where the longshore transport rate, Q_{LT} , in terms of m^3/s is given by the following equation:

$$Q_{LT} = \frac{S_N D_{50}^3}{(1-n)T_m} \tag{1}$$

with T_m = mean wave period, n = sediment porosity, S_N = the number of units passing a given control section in one wave [23–27]. In case of beaches, units are sand grains.

The GSb morphodynamics model considers the following equation for the longshore transport rate Q :

$$Q = Q_{LT} - \frac{K_{GSb}}{8\left(\frac{\rho_s}{\rho} - 1\right)(1-n)\tan\beta 1.416^{5/2}} H_b^2 c_{gb} \cos(\theta_{bs}) \frac{\partial H_b}{\partial x} \tag{2}$$

with ρ_s = density of sediment, ρ = density of water, $\tan\beta$ = average bottom slope, H_b = breaking wave height, c_{gb} = group celerity at breaking, θ_{bs} = wave obliquity at breaking. The breaking wave height is considered as a wave forcing. For more references, see [33,34].

The second term in Equation (2), i.e., the term:

$$\frac{K_{GSb}}{8\left(\frac{\rho_s}{\rho} - 1\right)(1-n)\tan\beta 1.416^{5/2}} H_b^2 c_{gb} \cos(\theta_{bs}) \frac{\partial H_b}{\partial x} \tag{3}$$

accounts for the longshore current and associated sediment transport induced by the alongshore gradient in wave height [35,36]. The average bottom slope is determined assuming cross transects of the bathymetric charts.

The GSb model presents one calibration coefficient solely, K_{GSb} , which does not depend on the grain size diameter and depends on the alongshore gradient in breaking wave height [23]. The general formula/procedure considers an energy flux approach combined with an empirical/statistical relationship between the wave-induced forcing and the number of moving units. GSb model allows to determine short-term (daily base) or long-term (yearly base) shoreline change for arbitrary combinations and configurations of structures (groynes, jetties, detached breakwaters and seawalls) and beach fills that can be represented on a modelled reach of coast.

To model the longshore sediment transport with the GSb numerical model, the 2 km long analysed shoreline has been divided in three cells and 6 sectors. The cells are indicated as the West cell, the VVIP cell, in the centre, and St. Regis cell at the eastern boundary of the beach. The sectors divide the West cell, the St. Regis cell and the area between groynes 3 and 4 each one in half and they have been used as a reference for the computation of the maximum accretion/erosion areas along the beach. Figure 4 shows the adopted initial design scenario, the cells and the reference sectors.

The actual adopted solution by the contracting company, involves the construction of four groynes: groyne 1 is 287 m long and reaches water depth 2.5 m; and groynes 2, 3 and 4 are, respectively, 230 m, 263 m and 287 m long and reach water depth 2.6 m, 3.3 m and 3.1 m. The intervention comprises a large

initial nourishment to create an area suitable for human beach recreational facilities and to increase the longevity of the beach. The sand will be taken from stockpiles in the south of Saadiyat island.

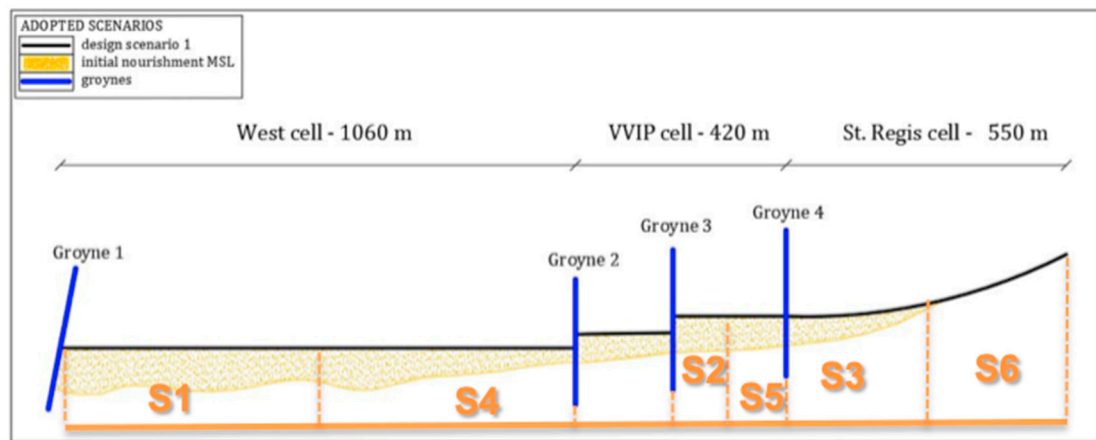


Figure 4. Schematic initial design scenario. Indicated are also the reference sectors for the computation of the maximum accretion/erosion along the beach.

2.3.3. Calibration of the GSB Model

The alongshore model computational domain has been assumed equal to 2000 m. The model grid cell resolution, DX , has been set equal to 40 m with a total number of cells, NX , equal to 50, whereas the model experiment has been carried out adopting a calculation time step, DT , equal to 1 h. GSB boundaries have been selected as pinned beach, meaning that the shoreline does not change over time in the extremes of the domain [23].

The closure depth, h_c [1], has been calculated by the following equation:

$$h_c = 2.28 H_s - 68.5 \left(H_{s,0-12}^2 / g T_{s,0-12}^2 \right) \quad (4)$$

where $H_{s,0-12}$ is the significant wave height exceeded for 12 h in one year and $T_{s,0-12}$ is the associated wave period; g is the gravitational acceleration. The closure depth has been calculated by means of the NOAA offshore wave data (at the grid node with coordinates 25° N and 54° E, indicated in Figure 3) at 16 m water depth. The calculated closure depth results equal to 3.6 m.

The estimation of the longshore sediment transport calibration coefficient, K_{GSb} , has been obtained based on the available historical data. It is worth to point out that the K_{GSb} does not depend on the grain size, while it depends on the characteristics of wave propagation. Two available Google Earth satellite images, from the years 2008 and 2009, have been considered to set the initial/final shoreline position and to determine the optimal value for the calibration coefficient. Different values of K_{GSb} , ranging between 0.005 and 0.5 have been adopted; for each of them, a measure of the error between the resulting calculated 2009 shoreline and the actual one has been determined, with a similar procedure as in [37]. The minimum value of the error is related to the optimal value for the calibration coefficient K_{GSb} , which has been assumed equal to 0.3. Figure 5 shows the 2008 and 2009 satellite shorelines and the shoreline resulting from the GSB calibration procedure. The resulting Root Mean Square Difference (RMSD) value is also shown in Figure 5, together with the distribution of the difference between the 2009 shoreline and the GSB model output (with $K_{GSb} = 0.3$) and the difference of the two 2008 and 2009 shorelines.

A period of one year has been simulated, from 1 January 2008 to 31 December 2008, considering the wave time series resulting from [10] with NOAA climate forecast system reanalyses dataset input winds (years 1979–2009) as input data (indicated as NOAA nearshore in Figure 3).

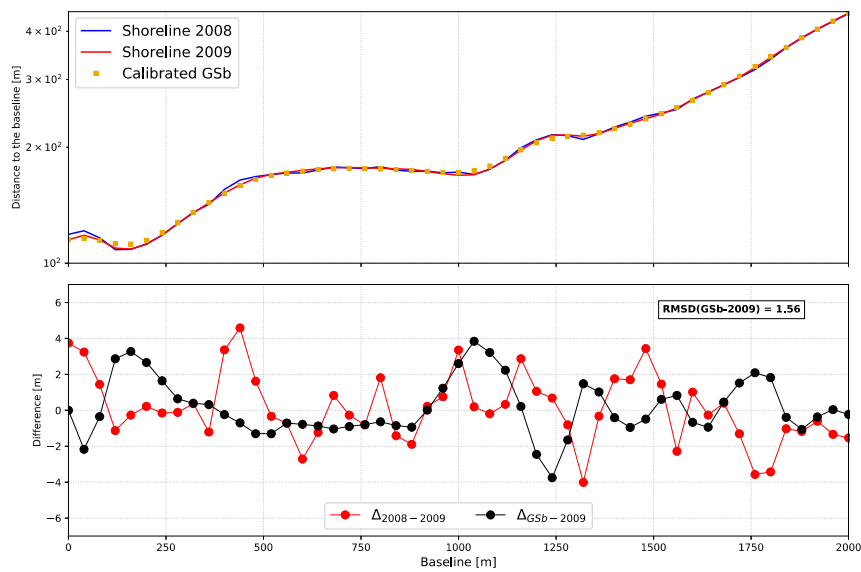


Figure 5. Top: historical shorelines adopted for the calibration of the General Shoreline beach (GSb) model; bottom: distribution of the difference between the 2009 shoreline and the GSb model output (with $K_{GSb} = 0.3$) and the difference of the two 2008 and 2009 Google Earth shorelines.

2.4. Other Numerical Models: Ghost

In the present work, use is also made of a well-established wave propagation numerical model, Ghost [38–40], which is a half plane and steady state marginal directional wave spectral transformation model solving the wave action conservation equation with an implicit finite-difference method on a rectilinear grid. The marginal directional spectrum for the wave transformation is a directional wave spectrum integrated in the frequency range [39,40]. The model is capable of simulating wave-structure and wave-current interactions: in particular, the combined effects of wave reflection, wave breaking, diffraction, shoaling, refraction and wave transmission through and over submerged structures. A more extended description of the Ghost model and also a comparison of the performances of Ghost with respect to other wave propagation numerical models such as STWave (Steady-State Spectral Wave Mode), for example for the propagation of waves in coastal inlets, can be found in [41], where the authors found that, overall, wave direction estimates from Ghost in inlets and near structures compared slightly better with measurements with respect to the STWave performances.

2.5. The Nourishment Performance Index

In the present work, a nourishment performance index (NPI) is defined, considering the maximum recession that will occur after 1/5 year from the nourishment intervention related to the initial volume of sand necessary for the nourishment, according to:

$$NPI = \frac{W}{S_{1yr} \cdot h_c} \tag{5}$$

where W is the initial design volume necessary for the nourishment, S_{1yr} is the area in recession in the emerged beach after 1 year, with respect to the initial shoreline and h_c the closure depth.

3. Results

3.1. Nearshore Wave Climate

The nearshore wave climate has been calculated in terms of significant wave height, H_s , wave peak period, T_p and mean wave direction, θ_i , at eight virtual buoys near the coast at different depths. Figure 6 shows the location of the virtual buoys, chosen in order to analyse the wave effects along the entire beach, with a focus in the proximity of the study area at the western side of the beach.

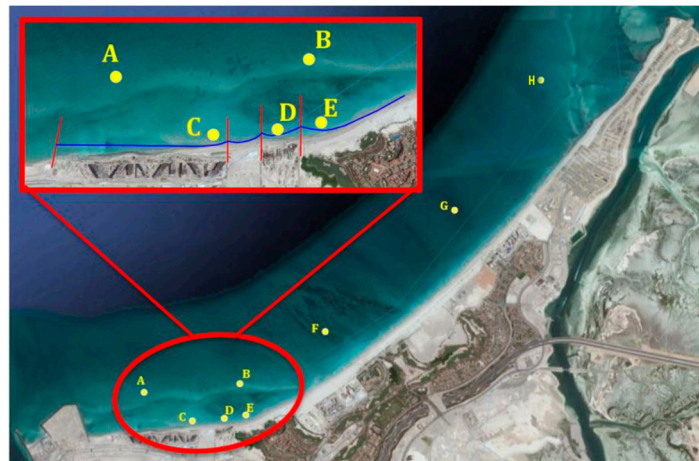


Figure 6. Positions of the virtual buoys along Saadiyat beach.

Results are reported in terms of wave rose plots indicating the wave appearance frequencies. Figure 7 shows the corresponding wave roses at the virtual buoys indicated in Figure 6 with labels from A to H: the influence of the bottom (seabed) determines a dissipation of the waves close to the beach. Results show that the most frequent wave’s events have directions in the sector 270° N–360° N, with a dominant North-West component, and maximum wave height lower than 1.8 m.

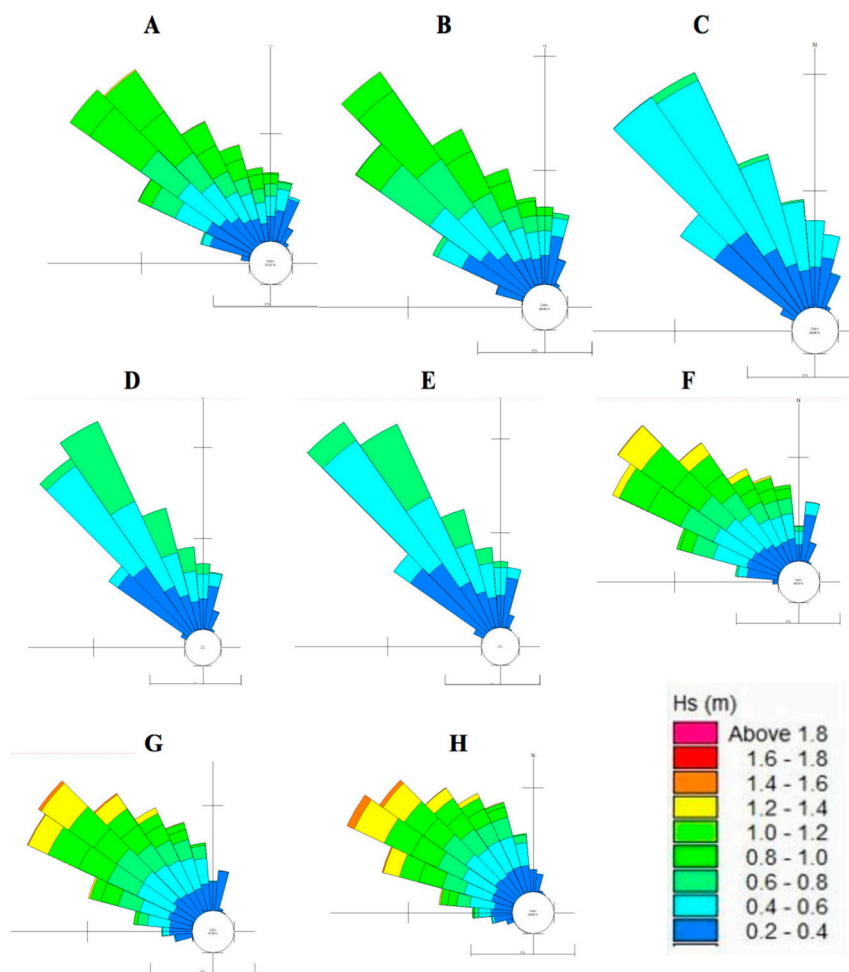


Figure 7. Wave climate at the eight virtual buoys, indicated as A–H in Figure 6, along Saadiyat beach.

Wave roses corresponding to virtual buoys C, D and E in Figure 6 are, indeed, similar when considering the main wave direction and Hs values. In particular, it can be noticed how changes of the coastline shape and the presence of groynes, acting as defence structures, obstruct the wave propagation, resulting in a wave energy reduction in C, D, and E with respect to the waves corresponding to A and B.

Results relative to the remaining virtual buoys show a good exposure of the beach to different wave conditions, i.e., the position of the virtual buoys has been chosen well enough so that the simulated beach conditions are sensitive to the action of the waves coming from all the possible directions; therefore, the climate at the virtual buoys is well representative of the real conditions of the beach. The bottom friction, the bathymetry of the area and the alignment of the beach determine a slight rotation of the fronts and only the directions from east to south are lost with respect to the original wave climate at the bathymetry 6 m.

3.2. Shoreline Design Scenarios

To increase the longevity of the beach and propose a sustainable solution over the years, some possible alternatives have been simulated. In particular, a different orientation of the as-built shoreline and different volume of sand for the nourishment have been tested. Figure 8 shows the scenarios with different orientations of the initial design shoreline. Based on the results of the sediment analysis (Section 2.1), it is assumed that the area of interest is characterised by medium sand with the median grain size $D_{50} = 0.26$ mm and the sorting parameter $D_{15}/D_{85} = 2.44$ (where: D_{15} (transition layer) is the 15th percentile particle size in the transition layer material, meaning that 15% of the sand is smaller than D_{15} mm, and D_{85} (filter media) is the 85th percentile particle size in the filter media).

In scenario 1, the initial alignment of the design shoreline is obtained from the nourishment of the entire stretch of coast. In particular, 600,000 m³ are necessary for the West cell, 240,000 m³ for the VVIP cell and 180,000 m³ for the St. Regis cell.

In the scenario 2, a rotation of the shoreline alignment for the west cell and the VVIP cell, respectively 5° and 10° counter clockwise, is proposed, with a consequent increase in the sand volume, which is necessary for the initial nourishment (respectively 830,000 m³ for the West cell and 270,000 m³ for the VVIP cell).

The difference of scenario 3 with respect to scenario 2 consists in the fact that the shoreline alignment in the West cell is around the centreline.

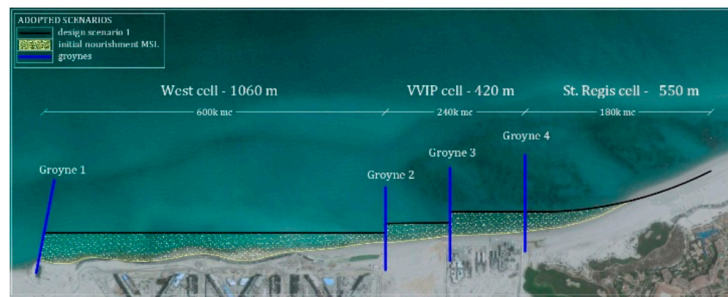
In the scenario 4, the initial shoreline alignment is the same as in scenario 1 but a counter clockwise rotation of 5° is expected for the West cell, from the centre of the cell to the groyne 2, with a relative increase in the nourishment sand requirement, from 600,000 m³ to 650,000 m³.

In the scenario 5, the shoreline alignment is similar to scenario 1, but a clockwise rotation of 5° has been imposed for the West cell, from the centre of the cell to the groyne 1. The volume of sand required is 50,000 m³ more than the volume foreseen in the scenario 1.

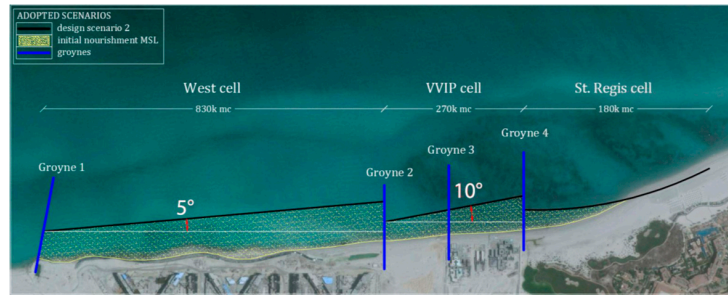
A summary of the volumes of sand needed for the initial nourishment in the different scenarios is reported in Table 3.

Table 3. Summary of the five design scenarios.

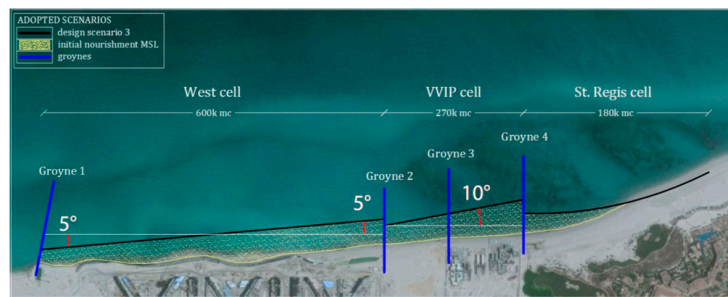
| Scenarios | Sand Volume (×10 ³ m ³) | | |
|-----------|--|-----------|----------------|
| | West Cell | VVIP Cell | St. Regis Cell |
| 1 | 600 | 240 | 180 |
| 2 | 830 | 270 | 180 |
| 3 | 600 | 270 | 180 |
| 4 | 650 | 240 | 180 |
| 5 | 650 | 270 | 180 |



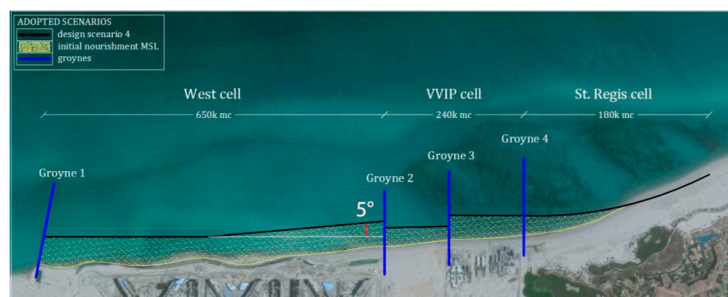
(A)



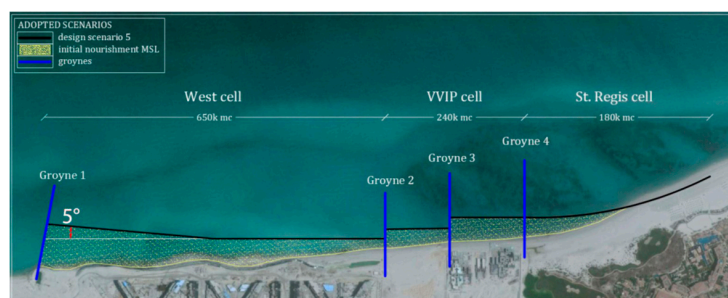
(B)



(C)



(D)



(E)

Figure 8. Schematic scenarios. (A) scenario 1; (B) scenario 2; (C) scenario 3; (D) scenario 4; (E) scenario 5.

3.3. Shoreline Evolution for the Design Scenarios

The shoreline evolution for each of the five considered scenarios has been modelled with the GSB model. The numerical simulations have been performed considering the evolution of the initial shoreline after 1 year, 2 years and 5 years from the end of the intervention.

Figure 9; Figure 10 show a comparison between the results for, respectively, the evolution in 1 year and in 5 years, in terms of maximum accretion/recession.

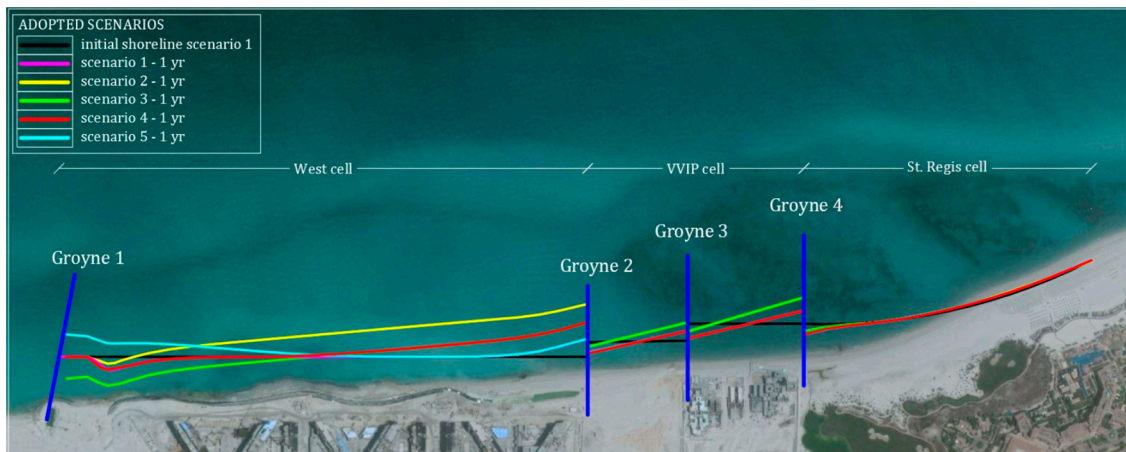


Figure 9. Evolution of the initial shoreline after 1 year, for the different considered the scenarios simulated.

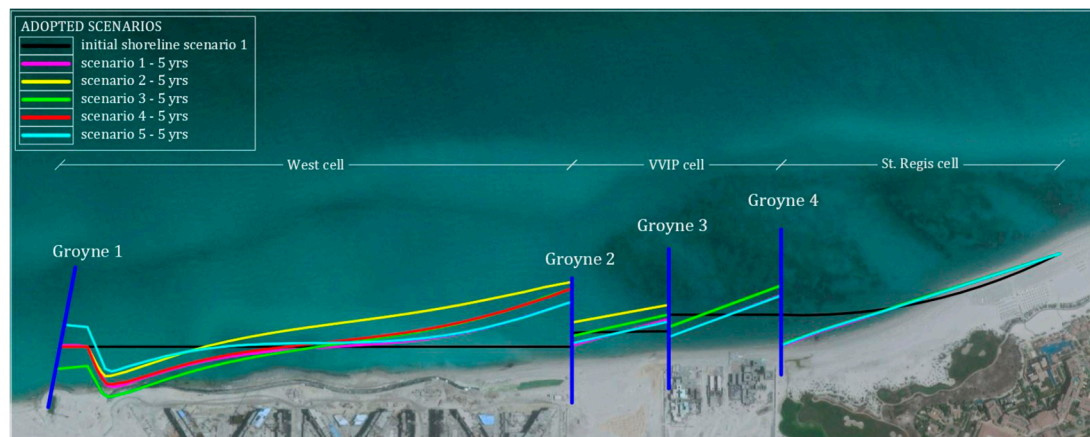


Figure 10. Evolution of the initial shoreline after 5 years, for the different considered scenarios.

The maximum accretion/recession volumes, i.e., the new beachline dry area as resulting from the shoreline shifts multiplied by the closure depth, in relation to the sand volume of the initial nourishment in the six sectors along the analysed shoreline, have been calculated. The shoreline shifts are calculated considering the new beach shoreline position as resulting after a fixed amount of time from the end of the intervention and the “as built shoreline after the nourishment intervention”. The results are shown in Tables 4 and 5.

Table 4. Maximum accretion/erosion occurred after 1 year, for the proposed scenarios.

| Scenarios | Sand Volume ($\times 10^3$ m ³) | | | Max Recession after 1 year (m) | | | Max Accretion after 1 year (m) | | |
|-----------|--|-----------|----------------|--------------------------------|----|----|--------------------------------|----|----|
| | West Cell | VVIP Cell | St. Regis Cell | S1 | S2 | S3 | S4 | S5 | S6 |
| 1 | 600 | 240 | 180 | 26 | 20 | 21 | 20 | 25 | 4 |
| 2 | 830 | 270 | 180 | 20 | 13 | 31 | 44 | 16 | 4 |
| 3 | 600 | 270 | 180 | 20 | 13 | 31 | 30 | 16 | 4 |
| 4 | 650 | 240 | 180 | 26 | 20 | 21 | 30 | 25 | 4 |
| 5 | 650 | 270 | 180 | 10 | 20 | 21 | 20 | 25 | 4 |

Table 5. Maximum accretion/erosion occurred after 5 years, for the proposed scenarios.

| Scenarios | Sand Volume ($\times 10^3$ m ³) | | | Max Recession after 5 years (m) | | | Max Accretion after 5 years (m) | | |
|-----------|--|-----------|----------------|---------------------------------|----|----|---------------------------------|----|----|
| | West Cell | VVIP Cell | St. Regis Cell | S1 | S2 | S3 | S4 | S5 | S6 |
| 1 | 600 | 240 | 180 | 80 | 27 | 62 | 75 | 39 | 14 |
| 2 | 830 | 270 | 180 | 65 | 22 | 77 | 71 | 29 | 14 |
| 3 | 600 | 270 | 180 | 63 | 22 | 77 | 79 | 24 | 14 |
| 4 | 650 | 240 | 180 | 79 | 27 | 62 | 79 | 39 | 14 |
| 5 | 650 | 270 | 180 | 85 | 27 | 61 | 76 | 39 | 14 |

3.4. The Nourishment Performance Index

The optimal intervention scenario among the five proposed has to be individuated on the basis of the NPI, calculated using Equation (5), considering the maximum recession that will occur for each of the considered scenarios after 1 year from the intervention at sector 1 (S1) (Figure 4), related to the initial volume of sand necessary for the nourishment, with W the initial design volume necessary for the nourishment of the West cell, $h_c = 3.6$ m, and S_{1yr} the area in recession in the emerged beach after 1/5 year, with respect to the initial shoreline. The areas in recession in the emerged beach result from the comparison of the original shoreline and the one simulated with GSb after 1 year or 5 years.

4. Discussion

From the results obtained in the present study, it has been found that the NPI allows selecting the optimal scenario based on the efficiency of the intervention. Table 6 shows the values of NPI for the different considered scenarios. In the first column, the initial sand volume W , necessary for the nourishment intervention is indicated. The second column shows the area of the beach that will be eroded 1 year or 5 years after the intervention, simulated with the GSb numerical model. This area is calculated as the area enclosed by the simulated shoreline after 1/5 years from the intervention and the corresponding initial shoreline for each scenario separately. The third column shows the calculated NPI values. The fourth column shows the increase in percentage of NPI in the beach longevity, calculated with respect to scenario 1, assumed as a reference.

Regarding the West cell and the results relative to 1 year, with respect to scenario 1, the result for scenario 2 shows an increase of NPI (+29%), which is due in a large part to a significant larger volume of sand (from 600,000 m³ to 830,000 m³). Scenario 3 can represent a good option because of the good longevity percentage increase (+15%) obtained, while keeping the same volume of sand necessary for the initial nourishment (600,000 m³). Scenario 4 shows almost the same NPI of scenario 1, but at the price of a slightly larger increase in the necessary sand volume for the nourishment (from 600,000 m³ to 650,000 m³).

Table 6. nourishment performance index (NPI) values at Saadiyat beach.

| West Cell | | | | | VVIP Cell | | | | | St. Regis Cell | | |
|-----------------------------|--|-----------------------------|-----|------------------|--|-----------------------------|-----|------------------|--|-----------------------------|-----|------------------|
| Recession (m ²) | Sand Volume ×10 ³ (m ³) | Recession (m ²) | NPI | NPI Increase (%) | Sand volume ×10 ³ (m ³) | Recession (m ²) | NPI | NPI Increase (%) | Sand Volume ×10 ³ (m ³) | | NPI | NPI Increase (%) |
| 1 | 600 | 2227 | 75 | reference | 240 | 2685 | 25 | reference | 180 | 1110 | 45 | reference |
| 2 | 830 | 2394 | 96 | 29 | 270 | 1707 | 44 | 77 | 180 | 638 | 78 | 74 |
| 3 | 600 | 1944 | 86 | 15 | 270 | 1338 | 56 | 126 | 180 | 693 | 72 | 60 |
| 4 | 650 | 2368 | 76 | 2 | 240 | 2712 | 25 | -1 | 180 | 962 | 52 | 15 |
| 5 | 650 | 874 | 207 | 176 | 270 | 2708 | 28 | 12 | 180 | 1140 | 44 | -3 |
| Scenarios (5 years) | Sand Volume ×10 ³ (m ³) | Recession (m ²) | NPI | NPI Increase (%) | Sand Volume ×10 ³ (m ³) | Recession (m ²) | NPI | NPI Increase (%) | Sand Volume ×10 ³ (m ³) | Recession (m ²) | NPI | NPI Increase (%) |
| 1 | 600 | 15,450 | 11 | reference | 240 | 3643 | 18 | reference | 180 | 6175 | 8 | reference |
| 2 | 830 | 13,920 | 17 | 54 | 270 | 1642 | 46 | 150 | 180 | 5625 | 9 | 10 |
| 3 | 600 | 13,017 | 13 | 19 | 270 | 1958 | 38 | 109 | 180 | 5737 | 9 | 8 |
| 4 | 650 | 14,106 | 13 | 19 | 240 | 3615 | 18 | 1 | 180 | 5683 | 9 | 9 |
| 5 | 650 | 13,798 | 13 | 21 | 270 | 3769 | 20 | 9 | 180 | 5856 | 9 | 5 |

For the West cell and the 1 year simulation, scenario 5 presents the larger NPI increase, equal to +176%. This is not verified for the remaining cells and considering the results relative to 5 years; the scenario that offers the overall best nourishment performance is scenario 2. Estimate of the nourishment performance is not extended to the entire project lifetime but it is limited to 5 years. This limit is chosen because at this time, the nourished shoreline retreats at some transects reaching an unacceptable threshold for the touristic, aesthetic and recreational uses of the beach.

Consequently, comparison of different design scenarios has showed that the NPI value depends mainly on the as built nourishment shoreline. The recommended scenario (i.e., scenario 2) durability is sounding.

This interesting and potentially very useful methodology can be adopted for analysing and predicting shoreline development under different coastal engineering interventions. The need for such a methodology arises from the large number of coastal interventions that are planned in high number worldwide and from the need to protect those from the climatically induced sea level rise and its hazardous consequences. The advantage of this definition is that all factors are measurable in-loco, are quantifiable by the development firms, are based on the physical characteristics of the beach (e.g., morphology), but also on aspects concerning the planned intervention (nourishments, longevity).

A potential benefit of this methodology is the fact that it also gives indication about the environmental sustainability (ES) of the planned interventions. In fact, ES, specifically the careful use of natural resources to preserve the ecosystems, is required in planning complex engineering interventions. ES is also an essential factor in mitigating the effects of environmental catastrophic phenomena, related to climate change. Since water covers up Earth's largest portion, it is a complex ecosystem; coastal engineers should include ES in the design of planned interventions.

The ES concept has been developed to ensure that in meeting its needs for water, food, shelter as well as engaging in leisure activities and entertainment where humanity does not cause damage to the environment or deplete resources that cannot be renewed [42]. However, despite many studies, the practices in coastal management have not yet reached a point where natural resources are being used sustainably.

In general, given the complexity of the environment and the ecosystem, environmental indexes could provide a useful tool to highlight environmental conditions and trends for policy purposes by isolating key aspects from an otherwise overwhelming amount of information [43]. Oftentimes, however, ES is difficult to translate in operational terms and many of the indexes proposed and mentioned above, include parameters, which are beyond the sphere of influence of local authorities/development firms [44]. This supports the scope of this study, i.e., to investigate an index to support also environmentally sustainable engineering applications.

Moreover, the NPI can be adopted not only as a valuable database for making management decisions, but also it encourages the local community and stakeholders to engage in the safeguard of the environment, given the simplicity of its definition and its immediate and easy application in real cases. This is a key aspect in ES-oriented engineering interventions: in fact, since ecological boundaries rarely meet up with political jurisdictions, it is necessary to be aware of major environmental issues and the best option to preserve the environment for future generations [45].

Specifically, the proposed NPI definition satisfies all the requirements for an environmental indicator to work well as a basis for policymaking [46]: (1) data availability; (2) ecosystem specificity of indicators; (3) spatial and conceptual aggregation of indicators and (4) baseline or reference values for indicators. The proposed NPI definition, the availability of data since the initial nourishment volume, the recession area and the closure depth are all easily measurable and well defined. The ecosystem specificity of the NPI is ensured through its dependence from the closure depth and the recession area, the aggregation is ensured by the NPI dependence from both environmental aspects (S_{1yr} and h_c) and specific aspects of the intervention (W) and the baseline is clearly drawn from scenario 1.

5. Conclusions

Environmental sustainability (ES) is an essential factor in solving environmental degradation; this is especially true when designing complex coastal engineering interventions.

The present paper describes the methodology followed to design a sustainable beach at Saadiyat Island, of the Abu Dhabi Municipality in the United Arab Emirates. Specifically, a proposed nourishment performance index appears suitable to quantify the level of sustainability for different coastal engineering interventions. The nourishment performance index is based on factors such as the initial volume necessary for the nourishment of the intervention area, the area in recession 1 year after the intervention and the closure depth.

The proposed methodology can be used for analysing and predicting shoreline development under different coastal engineering interventions. The need for such a methodology arises from the large number of coastal interventions that are planned in high number worldwide and from the need to protect those from the climatically induced sea level rise and its hazardous consequences. The advantage of this definition is that all factors are measurable in-*loco*, are quantifiable by the development firms and are based on the physical characteristics of the beach (e.g., morphology), but also on aspects concerning the planned intervention (nourishments, longevity).

Results show that the NPI value depends mainly on the as built nourishment shoreline. The recommended scenario (i.e., scenario 2) durability is sounding from the environmental sustainability prospective.

In conclusion, the application of the presented methodology in the evaluation of the impacts of the planned interventions at Saadiyat beach has been shown to be promising and can assist the engineers and/or environmentalists for designing/evaluating coastal interventions that are foreseen in the area.

Author Contributions: Conceptualization, W.H. and G.R.T.; methodology, G.R.T.; software, G.R.T., F.L., L.L. and A.F.; validation, F.L.; formal analysis, F.L. and A.F.; investigation, G.R.T.; resources, W.H.; data curation, L.L.; writing—original draft preparation, F.L.; writing—review and editing, G.R.T. and L.L.; visualization, F.L.; supervision, G.R.T.; project administration, W.H.; funding acquisition, W.H.

Funding: The present study is funded by the United Arab Emirates University research grant, through the National Water Centre, Grant #31R115; “Impact of coastal (long-shore) currents on erosion/deposition and consequent water/sediments quality variations along the coastal area of Abu Dhabi City”.

Acknowledgments: The authors thank the Abu Dhabi Municipality for providing in-situ data relative to wave conditions at Saadiyat beachfront.

Conflicts of Interest: The authors declare no conflict of interest.

References

- Hallermeier, R.J. A Profile Zonation for Seasonal Sand Beaches from Wave Climate. *Coast. Eng.* **1981**, *4*, 253–277. [[CrossRef](#)]
- Goda, Y. *Random Seas and Design of Maritime Structures*, 3rd ed.; Advanced Series on Ocean Engineering; World Scientific: Singapore, 2010.
- Tomasicchio, G.R.; D’Alessandro, F. Wave energy transmission through and over low crested breakwaters. *J. Coast. Res.* **2013**, *1*, 398–403. [[CrossRef](#)]
- USACE—United States Army, Corps of Engineers. *Shore Protection Manual*; Department of the Army, Waterways Experiment Station, Corps of Engineers, Coastal Engineering Research Center: Washington, DC, USA, 1984.
- Van der Meer, J.W. Rock Slopes and Gravel Beaches under Wave Attack. Ph.D. Thesis, Delft University of Technology, Delft, The Netherlands, 1988.
- Folk, R.L.; Ward, W.C. Brazos River Bar: A Study in the Significance of Grain Size Parameters. *J. Sediment. Petrol.* **1957**, *27*, 3–26. [[CrossRef](#)]
- Ojeda, E.; Ruessink, B.G.; Guillen, J. Morphodynamic response of a two-barred beach to a shoreface nourishment. *Coast. Eng.* **2008**, *55*, 1185–1196. [[CrossRef](#)]

8. Stauble, D.K. A review of the role of grain size in beach nourishment projects. In Proceedings of the National Conference on Beach Preservation Technology, Destin, FL, USA, 2–4 February 2005.
9. Utizi, K.; Corbau, C.; Rodella, I.; Nannini, S.; Simeoni, U. A mixed solution for a highly protected coast (Punta Marina, Northern Adriatic Sea, Italy). *Mar. Geol.* **2016**, *381*, 114–127. [[CrossRef](#)]
10. Hamza, W.; Lusito, L.; Ligorio, F.; Tomasicchio, G.R.; D’Alessandro, F. Wave Climate at Shallow Waters along the Abu Dhabi Coast. *Water* **2018**, *10*, 985. [[CrossRef](#)]
11. Saha, S.; Moorthi, S.; Pan, H.L.; Wu, X.; Wang, J.; Nadiga, S.; Tripp, P.; Kistler, R.; Woollen, J.; Behringer, D.; et al. The NCEP Climate Forecast System Reanalysis. *Bull. Am. Meteorol. Soc.* **2010**, *91*, 1015–1057. [[CrossRef](#)]
12. Amante, C.; Eakins, B.W. ETOPO1 1 Arc-Minute Global Relief Model: Procedures, Data Sources and Analysis. In *NOAA Technical Memorandum NESDIS; NGDC-24*; National Geophysical Data Center: Boulder, CO, USA, 2009; p. 19.
13. WAVEWATCH III 30-Year Hindcast Wave Model Developed by NOAA (Phase 2). Available online: <http://polar.ncep.noaa.gov/waves/hindcasts/nopp-phase2.php> (accessed on 4 October 2017).
14. The Climate Forecast System Reanalysis (1979–2010). Available online: <http://cfs.ncep.noaa.gov/cfsr/> (accessed on 4 October 2018).
15. Syvitski, J.P.M.; Slingerland, R.L.; Burgess, P.; Murray, A.B.; Wiberg, P.; Tucker, G.; Voinov, A. Morphodynamic models: An overview. In *River, Coastal and Estuarine Morphodynamics: RCEM 2009*; Vionnet, C.A., Garcia, M.H., Latruesse, E.M., Perillo, G.M.E., Eds.; Taylor & Francis: London, UK, 2010; pp. 3–20.
16. Short, A.D.; Jackson, D.W.T. Beach Morphodynamics. In *Treatise on Geomorphology*; Shroder, J.F., Ed.; Academic Press: San Diego, CA, USA, 2013; Volume 10, pp. 106–129.
17. Roelvink, D.; Reniers, A.; van Dongeren, A.; de Vries, J.V.T.; McCall, R.; Lescinski, J. Modelling storm impacts on beaches, dunes and barrier islands. *Coast. Eng.* **2009**, *56*, 133–1152. [[CrossRef](#)]
18. Hanson, H.; Kraus, N. *GENESIS—Generalised Model for Simulating Shoreline Change*; Report TR-CERC 89-19 (Report 1); Coastal and Hydraulic Laboratory, US Army Corps of Engineers: Washington, DC, USA, 1989.
19. Larson, M.; Kraus, N.C.; Hanson, H. Simulation of regional longshore sediment transport and coastal evolution—The “CASCADE” model. *Coast. Eng.* **2002**, *2002*, 2612–2624. [[CrossRef](#)]
20. GenCade Website. U.S. Army Corps of Engineers. Available online: <http://cirp.usace.army.mil/products/gencade.php> (accessed on 19 April 2019).
21. LITPACK Website. Danish Hydraulics Institute. Available online: <https://www.mikepoweredbydhi.com/products/litpack> (accessed on 19 April 2019).
22. Delft3D Website. Deltares, NL. Available online: <https://oss.deltares.nl/web/delft3d> (accessed on 19 April 2019).
23. Frey, A.E.; Connell, K.J.; Hanson, H.; Larson, M.; Thomas, R.C.; Munger, S.; Zundel, A. *GenCade Version 1 Model Theory and User’s Guide*; Technology Report ERDC/CHL TR-12-25; U.S. Army Engineer Research and Development Center: Vicksburg, MS, USA, 2012.
24. Dean, R.G. Equilibrium beach profiles: Characteristics and applications. *J. Coast. Res.* **1990**, *71*, 53–84.
25. Bruun, P. *Coast Erosion and the Development of Beach Profiles*; US Army Engineer Waterways Experiment Station; Beach Erosion Board Technical Memo: Vicksburg, MA, USA, 1954.
26. Lamberti, A.; Tomasicchio, G.R. Stone mobility and abrasion on reshaping breakwaters. In Proceedings of the Hornafjörður International Coastal Symposium, Höfn, Iceland, 20–24 June 1994; pp. 723–735.
27. Lamberti, A.; Tomasicchio, G.R. Stone mobility and longshore transport at reshaping breakwaters. *Coast. Eng.* **1997**, *29*, 263–289. [[CrossRef](#)]
28. Tomasicchio, G.R.; Archetti, R.; D’Alessandro, F.; Sloth, P. Long-shore transport at berm breakwaters and gravel beaches. In Proceedings of the International Conference Coastal Structures, Venice, Italy, 2–4 July 2007; pp. 65–76.
29. Tomasicchio, G.R.; D’Alessandro, F.; Barbaro, G.; Malara, G. General longshore transport model. *Coast. Eng.* **2013**, *71*, 28–36. [[CrossRef](#)]
30. Tomasicchio, G.R.; D’Alessandro, F.; Barbaro, G.; Musci, E.; De Giosa, T.M. Longshore transport at shingle beaches: An independent verification of the general model. *Coast. Eng.* **2015**, *104*, 69–75. [[CrossRef](#)]
31. Tomasicchio, G.R.; D’Alessandro, F.; Barbaro, G.; Ciardulli, F.; Francone, A.; Mahmoudi Kurdistani, S. General model for estimation of longshore transport at shingle/mixed beaches. In Proceedings of the 35th International Conference on Coastal Engineering, Antalya, Turkey, 17–20 November 2016.
32. Tomasicchio, G.R.; D’Alessandro, F.; Frega, F.; Francone, A.; Ligorio, F. Recent improvements for estimation of longshore transport. *Ital. J. Eng. Geol. Environ.* **2018**. [[CrossRef](#)]

33. Whitford, D.J.; Thornton, E.B. Comparison of wind and wave forcing of longshore currents. *Cont. Shelf Res.* **1993**, *13*, 1205–1218. [[CrossRef](#)]
34. Baldock, T.E.; Huntley, D.A. Long-wave forcing by the breaking of random gravity waves on a beach. Proceedings of the Royal Society of London. *Series A Math. Phys. Eng. Sci.* **2002**, *458*. [[CrossRef](#)]
35. Abessolo Ondo, G.; Bonou, F.; Tomety, F.S.; du Penhoat, Y.; Perret, C.; Degbe, C.G.E.; Almar, R. Beach Response to Wave Forcing from Event to Inter-Annual Time Scales at Grand Popo, Benin (Gulf of Guinea). *Water* **2017**, *9*, 447. [[CrossRef](#)]
36. Ozasa, H.; Brampton, A.H. Mathematical modeling of beaches backed by seawalls. *Coast. Eng.* **1980**, *4*, 47–64. [[CrossRef](#)]
37. Medellín, G.; Torres-Freyermuth, A.; Tomasicchio, G.R.; Francone, A.; Tereszkievicz, P.A.; Lusito, L.; Palemón-Arcos, L.; López, J. Field and Numerical Study of Resistance and Resilience on a Sea Breeze Dominated Beach in Yucatan (Mexico). *Water* **2018**, *10*, 1806. [[CrossRef](#)]
38. Carci, E.; Rivero, F.J.; Burchart, H.Y.; Maciñeira, E. The use of numerical modeling in the planning of physical model tests in a multidirectional wave basin. In Proceedings of the 28th International Coastal Engineering Conference, Cardiff, UK, 7–12 July 2002; pp. 485–494.
39. Rivero, F.J.; Arcilla, A.S.; Carci, E. Implementation of diffraction effects in the wave energy conservation equation. In Proceedings of the IMA Conference on Wind-Over-Waves Couplings: Perspectives and Prospects, Salford, UK, 8–10 April 1997.
40. Rivero, F.J.; Arcilla, A.S.; Carci, E. An analysis of diffraction in spectral wave models. In Proceedings of the 3rd International Symposium of Ocean Wave Measurement and Analysis, Waves 97, Reston, Virginia Beach, VA, USA, 3–7 November 1997; pp. 431–445.
41. Lin, L.; Demirbilek, Z. Evaluation of Two Numerical Wave Models with Inlet Physical Model. *J. Waterw. Port Coast. Ocean Eng.* **2005**, *131*, 149–161. [[CrossRef](#)]
42. IISD—International Institute of Sustainable Development. *Our Common Future*; Report of the World Commission on Environment and Development; IISD: New York, NY, USA, 1987.
43. Pantusa, D.; D’Alessandro, F.; Riefolo, L.; Principato, F.; Tomasicchio, G.R. Application of a Coastal Vulnerability Index. A Case Study along the Apulian Coastline, Italy. *Water* **2018**, *10*, 1218.
44. SUSTAIN Project. *Measuring Coastal Sustainability*; A Guide for the Self-Assessment of Sustainability Using Indicators and a Means of Scoring Them; Project Report; Coastal and Marine Union—EUCC: Leiden, The Netherlands, 2010; p. 32.
45. Fraser, E.D.; Dougill, A.J.; Mabee, W.E.; Reed, M.; McAlpine, P. Bottom up and top down: Analysis of participatory processes for sustainability index identification as a pathway to community empowerment and sustainable environmental management. *J. Environ. Manag.* **2006**, *78*, 114–127. [[CrossRef](#)] [[PubMed](#)]
46. Niemeijer, D. Developing Indicators for environmental policy: Data-driven and theory-driven approaches examined by example. *Environ. Sci. Policy* **2002**, *5*, 91–103. [[CrossRef](#)]

